IL NUOVO CIMENTO **47 C** (2024) 84
DOI 10.1393/ncc/i2024-24084-1

Colloquia: IFAE 2023

Impact of dimension-six EFT operators on triboson processes at the LHC(*)

C. Tarricone(1)(2)(**)

(1) *INFN, Sezione di Torino - Torino, Italy*
(2) *Dipartimento di Fisica, Università degli Studi di Torino - Torino, Italy*

received 13 February 2024

Summary. — A parton-level analysis exploring potential manifestations of new physics phenomena beyond the Standard Model in triboson production processes is presented. In the context of Standard Model Effective Field Theories, the sensitivity to anomalous kinematic effects stemming from the presence of dimension-six operators is evaluated. The results provide valuable insights into the electroweak sector of the Standard Model and potential indications of new physics.

1. – Introduction

The Standard Model Effective Field Theory (SM-EFT) framework provides a description of the effects of new physics via higher-dimensional operators. The SM-EFT Lagrangian expands upon the SM, introducing operators modifying the scattering matrix amplitudes, leading to observable event yields. The contribution in the Lagrangian of each dimension-n EFT operator, $Q_i^{(n)}$, is weighted by the respective Wilson coefficients, $c_i^{(n)}$, over a power n-4 of a new physics scale, Λ, resulting in

$$\mathcal{L}_{\text{SM-EFT}} = \mathcal{L}_{\text{SM}}^{(4)} + \sum_{i,n} \frac{c_i^{(n)}}{\Lambda^{n-4}} Q_i^{(n)}. \tag{1}$$

Considering only the effect of dimension-six operators, it brings to a modification in the total event yield, which results in the sum of an SM contribution, a linear interference term between the SM diagrams and a single operator, the pure BSM contribution, quadratically scaling with the Wilson coefficient, and the mixed interference term between pairs of (same-dimension) operators.

(*) IFAE 2023 - "Energy Frontier" session
(**) Speaker on behalf of a collaboration between Torino (R. Bellan, A. Mecca, C. Tarricone and A. Vagnerini) and Milano-Bicocca (G. Boldrini, F. Cetorelli, P. Govoni and A. Massironi) working groups.

TABLE I. – *Dependency of the studied processes on the bosonic EFT operators. Empty cells indicate the absence of diagrams affected by a particular operator for that channel. The brackets indicate operators that introduce anomalies in the studied channels, but these effects are strongly suppressed by the kinematic selection criteria. Hence, for the purpose of this study, these operators are neglected for the corresponding channels.*

	Q_W	Q_{HB}	Q_{HW}	Q_{HWB}	Q_{HD}	$Q_{H\Box}$
WZγ	X	X	X	X	X	
ZZγ		X	X	X	X	
VZγ	X	X	X	X	X	
QCD-Zγjj				X	X	
VZZ	X	(X)	X	X	X	(X)
QCD-ZZjj				X	X	

The triboson analyses traditionally neglect the dimension-six operators' potential effects focusing on the dimension-eight operators' impact on quartic couplings. The talk was based on ref. [1], that proved the potential impact of dimension-six operators on triple and quartic gauge vertices, along with Higgs-mediated diagrams, is not negligible for triboson production processes from 13 TeV proton-proton collisions at the LHC. In particular, the processes under study are the VZγ and VZZ production (V=W,Z). The W$^{\pm}$Zγ and ZZγ production processes are studied in the fully leptonic final states given by $\mu\nu_\mu\, e^+e^-\,\gamma$ and $\mu^+\mu^-\, e^+e^-\,\gamma$, respectively. They are also studied in an inclusive semi-leptonic channel, 2 jets + $l^+l^-\,\gamma$, where the jets in the final state are the product of hadronizing quarks coming from the V boson decay. The VZZ production process is studied in a semi-leptonic channel 2 jets + $\mu^+\mu^-\, e^+e^-$. For the semi-leptonic channels, the processes with jet pairs induced by QCD vertices, denoted as *QCD-ZZjj* / *QCD-Zγjj*, are also included as backgrounds.

The study focuses on the CP-even dimension-six bosonic operators of the Warsaw basis [2], excluding the ones inducing the gluon self-couplings and the anomalous couplings of gluons with the Higgs boson, namely Q_G and Q_{HG}, since they do not affect the electroweak sector. The resulting set of operators considered in this work, inducing diagrams for the processes of interest, is summarized in table I.

2. – Generation and shape analysis

The event generation is performed at the leading order using the amplitude decomposition technique with MADGRAPH5_AMC@NLO 2.6.5 [3] interfaced with the SMEFTSIM 3.0 package [4, 5]. Non-resonant diagrams are included (but kinematically suppressed), modeling all processes as full $2 \to 6$ fermions and $2 \to 4$ fermions + γ. The generation is also reproduced with the re-weighting technique to ensure the stability of the results in the profiled fit analysis for the semi-leptonic channels. A comprehensive description of both the amplitude decomposition and re-weighting techniques is provided in ref. [6].

Individual operator contributions and their interference are distinctly generated. The SM term is generated with all BSM dynamics set to zero. In the context of the one-dimensional study (one operator at a time) only contributions of individual operators are considered. In the two-dimensional case, the interference contribution between pairs

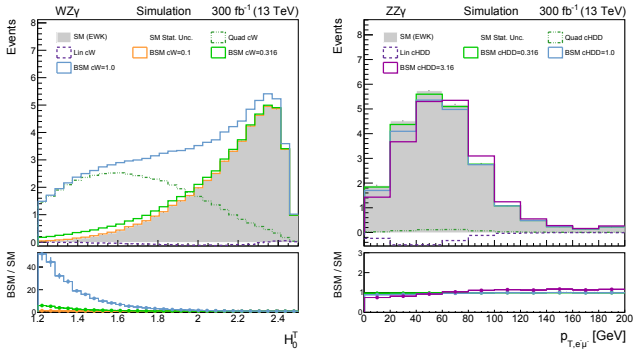

Fig. 1. – The plot on the left shows the distribution obtained for the Q_W operator affecting the WZγ production process as a function of the zero-th order Fox-Wolfram moment [8] H_0^T of the $3l\nu\gamma$ system, defined as $\sum_{a,b\in\{e^{\pm},\mu^{+},\gamma}\frac{p_T^a p_T^b}{(p_T^{Tot.})^2}$, where p_T^{ν} is the missing transverse energy per event. In this case, the shape of the EFT quadratic component is well resolved with respect to the SM one. The plot on the right shows the impact on the transverse momentum $p_T^{e^-\mu^-}$ of the same-sign charged leptons of the EFT components induced by the operator Q_{HD} affecting the ZZγ production process. It is an example of non-negligible destructive interference of the Q_{HD}-induced diagrams with the SM component, that partially mitigated by the presence of the positive-definite quadratic component. Taken from Bellan R. *et al.*, *JHEP*, **2023** (2023) 158, `https://doi.org/10.1007/JHEP08(2023)158`, published under the terms of the Creative Commons Attribution License `https://creativecommons.org/licenses/by/4.0/`.

of operators is additionally considered. The interference terms between all the possible operator pairs in the specified subset are computed to derive the profiled constraints.

The analysis is conducted under the assumption of CP symmetry conservation, $U(3)^5$ flavor symmetry, and $\{m_W, m_Z, G_F\}$ as the input parameter scheme [7]. The event selection applied is based on the phase space regions outlined in table 4 of ref. [1], where the variables studied are also listed channel by channel.

Figure 1 shows two examples of distributions investigated. More examples of variables examined can be found in ref. [1]. The shape analysis allows the identification of a phase-space region where to isolate the potential EFT effects.

3. – One-dimensional expected constraints on the Wilson coefficients

The expected bounds on the Wilson coefficients associated with the operators under scrutiny are evaluated at the generator level for an integrated luminosity of 300 fb^{-1}. A likelihood scan is performed over the values of the Wilson coefficient c_i in a fixed range, for each channel, from the distributions of all the variables of interest. This procedure is computed for each variable of interest using the Combine tool [9]. A comprehensive description of the likelihood scan construction is provided in ref. [1, 6]. From the likelihood scans, the 68%(95%) confidence level intervals in the c_i estimates are extracted by requiring $-2\Delta\log\mathcal{L} < 1(3.84)$ [10], where $\mathcal{L}$ is the likelihood function. The confidence intervals for the considered Wilson coefficients are evaluated neglecting theoretical and experimental systematic uncertainties, with the exception of the luminosity uncertainty of 2%, which affects the statistical precision of the results. The more stringent the estimated constraints, the higher is the sensitivity to the kinematic anomalies induced by the corresponding EFT operator. The global analysis of the sensitivity estimate is

TABLE II. – *Confidence intervals on the estimates of the subset of Wilson coefficients considered, extracted from the respective likelihood scan for the most sensitive variable, for each channel studied. The last rows the confidence intervals obtained combining all the triboson channels involving diagrams induced by operators individually included in the SM Lagrangian, compared to the results coming from a VBS combination in the study of ref.* [6] *combining many VBS channels. The results are referred to a benchmark integrated luminosity of 300 fb^{-1}. Taken from* BELLAN R. *et al., JHEP,* ***2023*** *(2023) 158,* `https://doi.org/10.1007/JHEP08(2023)158`*, published under the terms of the Creative Commons Attribution License* `https://creativecommons.org/licenses/by/4.0/`.

Processes	Op.s →	Q_W	Q_{HB}	Q_{HW}	Q_{HWB}	Q_{HD}
WZγ	Best var.	p_T^{l1}	$p^{\gamma}_{T(Z)}$	$p^{\gamma}_{T(Z)}$	$p^{\gamma}_{T(Z)}$	$p^{l1}_{T(WZ)}$
	68% C.L.	[-0.20,0.21]	[-0.41,0.41]	[-0.44,0.44]	[-0.50,0.73]	[-1.36,1.79]
	95% C.L.	[-0.31,0.32]	[-0.60,0.60]	[-0.65,0.65]	[-0.79,1.04]	[-2.50,11.2]
ZZγ	Best var.		$p^{\gamma}_{T(Z_1)}$	$m_{\mu\mu}$	$m_{\mu\mu}$	$p_T^{e^+\mu^+}$
	68% C.L.	No	[-0.62,0.61]	[-0.68,0.68]	[-0.81,1.06]	[-1.91,4.55]
	95% C.L.	diagrams	[-0.90,0.90]	[-0.98,0.99]	[-1.23,1.49]	[-3.27,6.53]
VZγ	Best var.	p_T^{l1}	m_{jj}	m_{jj}	$p^{l1}_{T(\gamma)}$	$p^{l2}_{T(\gamma)}$
	68% C.L.	[-0.26,0.26]	[-0.55,0.54]	[-0.60,0.60]	[-0.11,0.11]	[-0.17,0.17]
	95% C.L.	[-0.37,0.37]	[-0.77,0.76]	[-0.84,0.84]	[-0.22,0.23]	[-0.33,0.34]
VZZ	Best var.	p_T^{l1}		p_T^V	$m_{\mu\mu}$	$p_T^{e^+\mu^+}$
	68% C.L.	[-0.63,0.63]	Negligible	[-4.78,4.08]	[-0.80,0.65]	[-2.73,1.82]
	95% C.L.	[-0.97,0.97]		[-6.91,6.17]	[-2.22,1.20]	[-3.78,2.82]
VZZ/VZγ comb.	68% C.L.	[-0.18,0.19]	[-0.37,0.37]	[-0.40,0.40]	[-0.11,0.11]	[-0.17,0.17]
	95% C.L.	[-0.27,0.28]	[-0.53,0.53]	[-0.57,0.57]	[-0.21,0.21]	[-0.33,0.33]
VBS	95% C.L.	[-0.19,0.18]	-	[-1.02,1.08]	[-1.34,0.96]	[-1.98,1.74]

obtained by combining all the triboson production channels for the common operators. The best variable is identified by the sensitivity bounds at 68% confidence level. Table II summarizes the results of the one-dimensional scan. The sensitivity estimates for the semi-leptonic channels, VZZ and VZγ, include the effects of the QCD-induced background processes.

4. – Simultaneous constraints on different Wilson coefficients

The analysis procedure is reproduced in the same way for the two-dimensional case, by inserting the operators pairwise into the fit. For each channel, the confidence regions are extracted from the likelihood scans using the variable most sensitive to the operator pair. The statistical combination of the likelihood is then performed for all the channels.

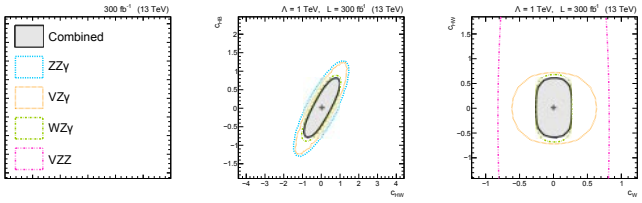

Fig. 2. – Bi-dimensional likelihood contour levels at $-2\Delta \log \mathcal{L} = 2.3$ from the triboson channels sensitive for the Q_{HB}-Q_{HW} and Q_W-Q_{HW} pairs of operators, respectively. In the case of the semi-leptonic channels VZZ and VZγ, the QCD-induced backgrounds and the corresponding EFT contributions are included into the fit. The central plot shows the case of two operators inducing the same anomalous couplings between the Higgs boson and the neutral gauge bosons, for which a linear correlation between the estimates of the corresponding Wilson coefficients can be observed. The latter is attributed to a large mutual interference term, since the linear interference terms with the SM are negligible. The right plot illustrates a case for which the potential anomalies induced by the Q_W operator in the considered processes can be regarded as uncorrelated with those caused by the other operators. Taken from Bellan R. *et al.*, *JHEP*, **2023** (2023) 158, `https://doi.org/10.1007/JHEP08(2023)158`, published under the terms of the Creative Commons Attribution License `https://creativecommons.org/licenses/by/4.0/`.

Some examples of the corresponding 68% C.L. areas are shown in fig. 2. The complete matrix of two-dimensional expected confidence regions associated with every possible couple of operators in the subset under study can be found in ref. [1].

A global fit constraining the individual coefficients is also performed. Limits on a single Wilson coefficient are derived by profiling all the other considered coefficients. Floating parameters are treated as unconstrained nuisances with a flat prior. The comparison between the profiled and individual constraints at 95% C.L. for each Wilson coefficient is shown in fig. 3. An expected decrease in the sensitivity of the profiled fit with respect to the individual constraints can be observed for the combination of all the triboson channels under study. This effect is more pronounced for the EFT operators affecting the couplings between Higgs and gauge bosons. This can be explained by the presence of anomalies induced in the same vertices, leading to flat directions and large mutual interferences. The only exceptions are the anomalous effects induced by Q_W, uncorrelated with the other operators, as observed in the two-dimensional contours in fig. 2 for the $\{c_W, c_{HW}\}$ case.

5. – Summary and conclusions

The first benchmark study of the sensitivity of triboson measurements to dimension-six SM-EFT operators was presented, addressing the study of the triboson fully leptonic WZγ and ZZγ channels, and the semi-leptonic inclusive VZγ and VZZ channels, where V=W,Z. The study covers the main class of corrections affecting triple, quartic, and Higgs-gauge couplings, adopting a subset of the Warsaw basis CP-symmetric operators with $\{m_W, m_Z, G_F\}$ as input parameters. EFT components for all channels and operators were generated at the parton level up to the Λ^{-4} order. The sensitivity constraints are computed for a LHC measurement with proton-proton collisions at a center-of-mass energy of 13 TeV and for a projected total luminosity of 300 fb^{-1}.

The study reveals that the semi-leptonic VZγ channel is the most sensitive to bosonic operators. The leading lepton transverse momentum imposes strong constraints on anomalous triple and quartic gauge boson couplings, showcasing competitive sensitiv-

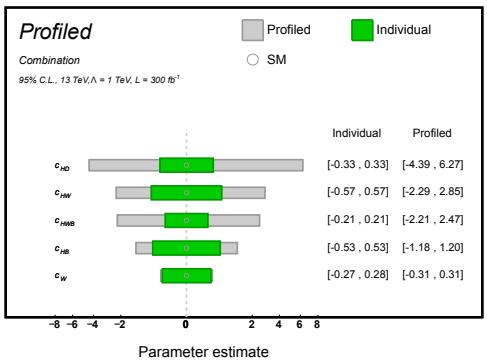

Fig. 3. – Comparison between the profiled and the individual expected constraints (quadratic scale) on the Wilson coefficients from the combination of the leptonic channels WZγ, ZZγ, and the semi-leptonic channels VZγ, VZZ. The solid dots denote the SM expectation. Gray-filled boxes indicate the 95% C.L. intervals obtained by estimating the corresponding Wilson coefficient as the parameter of interest, with all the other coefficients left floating in the maximum interval (-20,20). Green-filled boxes indicate the 95% C.L. individual constraints. Taken from Bellan R. *et al.*, *JHEP*, **2023** (2023) 158, `https://doi.org/10.1007/JHEP08(2023)158`, published under the terms of the Creative Commons Attribution License `https://creativecommons.org/licenses/by/4.0/`.

ity with existing literature on vector boson scattering analyses.

Results from the two-dimensional scan of operators illustrate complementarity and interplay between different measurements, highlighting orthogonal directions in sensitivity for different pairs of operators. The study also explores the impact of mutual interference terms in the fit, revealing linear (anti-)correlation in sensitivity to pairs of operators. Constraints on the individual Wilson coefficients are also extracted by profiling all the other coefficients in the set of interest. A non-negligible decrease of is highlighted by the profiled fit, but it does not compromise the constraining power of these analyses to the anomalies induced by dimension-six operators.

Possible improvements of the study presented include the refinement of this analysis to account for detector reconstruction effects and a more detailed treatment of reducible background processes. The scope of the investigation can be further expanded in the future through the development of new models considering the next terms in the amplitude of the scattering matrix, namely the linear interference term of dimension-eight operators with the SM diagrams, and the mixed interference between dimension-six and dimension-eight operators.

REFERENCES

[1] Bellan R. *et al.*, *J. High Energy Phys.*, **08** (2023) 158.
[2] Grzadkowski B. *et al.*, *J. High Energy Phys.*, **10** (2010) 085.
[3] Alwall J. *et al.*, *J. High Energy Phys.*, **07** (2014) 079.
[4] Brivio I. *et al.*, *J. High Energy Phys.*, **12** (2017) 070.
[5] Brivio I., *J. High Energy Phys.*, **04** (2021) 073.
[6] Bellan R. *et al.*, *J. High Energy Phys.*, **05** (2022) 039.
[7] Brivio I. *et al.*, CERN-LPCC-2021-002, 11 (2021).
[8] Fox G. C. and Wolfram S., *Nucl. Phys. B*, **149** (1979) 413.
[9] The CMS Collaboration, *Eur. Phys. J. C*, **75** (2015) 212.
[10] The Particle Data Group Collaboration, *Prog. Theor. Exp. Phys.*, **8** (2020) 083C01.